

The effect of supersymmetric CP phases on Chargino-Pair Production via Drell-Yan Process at the LHC

Kerem CANKOÇAK

Department of Physics, Mugla University, Mugla- Turkey

Aytekın AYDEMİR

Department of Physics, Mersin University, Mersin-Turkey

Ramazan SEVER

Department of Physics, Middle East Technical University, Ankara- Turkey

(November 16, 2018)

Abstract

We compute the rates for pp annihilation into chargino-pairs via Drell-Yan process taking into account the effects of supersymmetric soft phases, at proton-proton collider. In particular, the phase of the μ parameter gains direct accessibility via the production of dissimilar charginos. The phases of the trilinear soft masses do not have a significant effect on the cross sections.

PACS numbers:14.80.Ly, 12.15.Ji, 12.60.Jv

I. INTRODUCTION

Supersymmetry (SUSY), is one of the most favored extensions of the SM which is capable of stabilizing the Higgs sector of fundamental scalars against the ultraviolet divergences. The (soft) breaking of SUSY, around the TeV scale, brings about two new ingredients compared to the standard electroweak theory (SM): First, there are novel sources of flavor violation coming through the off-diagonal entries of the squark mass matrices. Second, there are novel sources of CP violation coming from the phases of the soft masses. The first effect, which cannot be determined theoretically, is strongly constrained by the FCNC data [1], and therefore, as a predictive case, it is convenient to restrict all flavor-violating transitions to the charged-current interactions where they proceed via the known CKM angles. However, this very restriction of the flavor violation to the SM one does not evade new sources of CP violation. Indeed, the model possesses various flavor-blind CP-odd phases contained in the complex μ parameter, A parameters, and gauge fermion masses M_i .

These phases form the new sources of CP violation which shows up in the electric dipole moments (EDMs) of leptons and hadrons (See [2] and references therein). For heavy quark EDMs see [3] and for the rate asymmetries of various heavy-light mesons [4]. Therefore, it is of fundamental importance to determine appropriate collider processes where all or some of the SUSY CP phases can be inferred or measured. In fact, the effects of the SUSY CP phases on the Higgs production has already been analyzed in [5,6]. In this work we will discuss the chargino-pair production at LHC energies and ways of isolating the phase of the μ parameter from the cross section.

Due to the large energy and high luminosity of incoming protons, LHC is a very useful machine to detect charginos. The dominant production mechanism for chargino pairs at a hadron collider is the quark-antiquark annihilation. In this sense, the number of chargino pair production events differ from pp to $p\bar{p}$ colliders. In what follows we will compute the cross section for $pp \rightarrow \tilde{\chi}_i^+ \tilde{\chi}_j^- + X$ as a function of $\varphi_\mu = \text{Arg}[\mu]$ for various values of $|\mu|$

and the SU(2) gaugino mass M_2 . As the analyses of EDMs [2,3] make it clear the effects of SUSY CP phases are expected to grow with lowering soft masses.

II. $Q\bar{Q} \rightarrow \tilde{\chi}_I^+ \tilde{\chi}_J^-$

Our analysis is similar to that used for the linear collider processes [7]. The relevant Feynman diagrams are depicted in Fig. 1. In what follows we mainly deal with the first two diagrams since the third one is suppressed by presumably heavy squarks. Then it is obvious that the amplitude for the process depends exclusively on the phases in the chargino sector, *i.e.*, the phase of the μ parameter.

Here we summarize the masses and couplings of the charginos for completeness (See [8] for details). The charginos which are the mass eigenstates of charged gauginos and Higgsinos are described by a 2×2 mass matrix

$$M_C = \begin{pmatrix} M_2 & \sqrt{2}M_W \cos \beta \\ \sqrt{2}M_W \sin \beta & |\mu|e^{i\varphi_\mu} \end{pmatrix} \quad (1)$$

where M_2 is the SU(2) gaugino mass taken to be real throughout the work. The masses of the charginos as well as their mixing matrices follow from the bi-unitary transformation

$$C_R^\dagger M_C C_L = \text{diag}(m_{\chi_1}, m_{\chi_2}) \quad (2)$$

where C_L and C_R are 2×2 unitary matrices, and m_{χ_1} , m_{χ_2} are the masses of the charginos χ_1 , χ_2 such that $m_{\chi_1} < m_{\chi_2}$. It is convenient to choose the following explicit parametrization for the chargino mixing matrices

$$C_L = \begin{pmatrix} \cos \theta_L & \sin \theta_L e^{i\varphi_L} \\ -\sin \theta_L e^{-i\varphi_L} & \cos \theta_L \end{pmatrix} \quad (3)$$

$$C_R = \begin{pmatrix} \cos \theta_R & \sin \theta_R e^{i\varphi_R} \\ -\sin \theta_R e^{-i\varphi_R} & \cos \theta_R \end{pmatrix} \cdot \begin{pmatrix} e^{i\phi_1} & 0 \\ 0 & e^{i\phi_2} \end{pmatrix} \quad (4)$$

where the angle parameters $\theta_{L,R}$, $\varphi_{L,R}$, and $\phi_{1,2}$ can be determined from the defining Eq. (1). A straightforward calculation yields

$$\begin{aligned}
\tan 2\theta_L &= \frac{\sqrt{8}M_W\sqrt{M_2^2\cos^2\beta + |\mu|^2\sin^2\beta + |\mu|M_2\sin 2\beta\cos\varphi_\mu}}{M_2^2 - |\mu|^2 - 2M_W^2\cos 2\beta} \\
\tan 2\theta_R &= \frac{\sqrt{8}M_W\sqrt{|\mu|^2\cos^2\beta + M_2^2\sin^2\beta + |\mu|M_2\sin 2\beta\cos\varphi_\mu}}{M_2^2 - |\mu|^2 + 2M_W^2\cos 2\beta} \\
\tan \varphi_L &= \frac{|\mu|\sin\varphi_\mu}{M_2\cot\beta + |\mu|\cos\varphi_\mu} \\
\tan \varphi_R &= -\frac{|\mu|\cot\beta\sin\varphi_\mu}{|\mu|\cot\beta\cos\varphi_\mu + M_2}
\end{aligned} \tag{5}$$

in terms of which the remaining two angles ϕ_1 and ϕ_2 read as follows

$$\tan \phi_i = \frac{\text{Im}[Q_i]}{\text{Re}[Q_i]} \tag{6}$$

where $i = 1, 2$ and

$$\begin{aligned}
Q_1 &= \sqrt{2}M_W[\cos\beta\sin\theta_L\cos\theta_R e^{-i\varphi_L} + \sin\beta\cos\theta_L\sin\theta_R e^{i\varphi_R}] \\
&\quad + M_2\cos\theta_L\cos\theta_R + |\mu|\sin\theta_L\sin\theta_R e^{i(\varphi_\mu + \varphi_R - \varphi_L)} \\
Q_2 &= -\sqrt{2}M_W[\cos\beta\sin\theta_R\cos\theta_L e^{-i\varphi_R} + \sin\beta\cos\theta_R\sin\theta_L e^{i\varphi_L}] \\
&\quad + M_2\sin\theta_L\sin\theta_R e^{i(\varphi_L - \varphi_R)} + |\mu|\cos\theta_L\cos\theta_R e^{i\varphi_\mu}.
\end{aligned} \tag{7}$$

The origin of the phases $\theta_{L,R}$, $\varphi_{L,R}$, and $\phi_{1,2}$ is easy to trace back. The angles θ_L and θ_R would be sufficient to diagonalize, respectively, the quadratic mass matrices $M_C^\dagger M_C$ and $M_C M_C^\dagger$ if M_C were real. As a result one needs the additional phases $\varphi_{L,R}$ which are identical to the phases in the off-diagonal entries of the matrices $M_C^\dagger M_C$ and $M_C M_C^\dagger$, respectively. However, these four phases are still not sufficient for making the chargino masses real positive due to the bi-unitary nature of the transformation, and hence, the phases ϕ_1 and ϕ_2 can not also be made real positive. Finally, inserting the unitary matrices C_L and C_R into the defining Eq. (1) one obtains the following expressions for the masses of the charginos

$$\begin{aligned}
m_{\chi_{1(2)}}^2 &= \frac{1}{2}\left\{M_2^2 + |\mu|^2 + 2M_W^2 - (+)[(M_2^2 - |\mu|^2)^2 + 4M_W^4\cos^2 2\beta\right. \\
&\quad \left.+ 4M_W^2(M_2^2 + |\mu|^2 + 2M_2|\mu|\sin 2\beta\cos\varphi_\mu)]^{1/2}\right\}.
\end{aligned} \tag{8}$$

The fundamental SUSY parameters M_2 , $|\mu|$, $\tan\beta$ and the phase parameter $\cos\varphi_\mu$ can be extracted from the chargino $\tilde{\chi}_{1,2}^\pm$ parameters [7] *i.e.* the masses $m_{\tilde{\chi}_{1,2}^\pm}$ and the two mixing angles ϕ_L and ϕ_R of the left and right chiral components of the wave function. These mixing angles are physical observables and they can be measured just like the chargino masses $m_{\tilde{\chi}_{1,2}^\pm}$ in the process $q + \bar{q} \rightarrow \tilde{\chi}_i^+ + \tilde{\chi}_j^-$. The two angles ϕ_L and ϕ_R and the nontrivial phase angles $\{\varphi_L, \varphi_R, \phi_1, \phi_2\}$ define the couplings of the chargino-chargino- Z vertices

$$\begin{aligned}
\langle \tilde{\chi}_{1L}^- | Z | \tilde{\chi}_{1L}^- \rangle &= -\frac{e}{s_W c_W} \left[s_W^2 - \frac{3}{4} - \frac{1}{4} \cos 2\theta_L \right] \\
\langle \tilde{\chi}_{1L}^- | Z | \tilde{\chi}_{2L}^- \rangle &= +\frac{e}{4s_W c_W} e^{-i\varphi_L} \sin 2\theta_L \\
\langle \tilde{\chi}_{2L}^- | Z | \tilde{\chi}_{2L}^- \rangle &= -\frac{e}{s_W c_W} \left[s_W^2 - \frac{3}{4} + \frac{1}{4} \cos 2\theta_L \right] \\
\langle \tilde{\chi}_{1R}^- | Z | \tilde{\chi}_{1R}^- \rangle &= -\frac{e}{s_W c_W} \left[s_W^2 - \frac{3}{4} - \frac{1}{4} \cos 2\theta_R \right] \\
\langle \tilde{\chi}_{1R}^- | Z | \tilde{\chi}_{2R}^- \rangle &= +\frac{e}{4s_W c_W} e^{-i(\varphi_R - \phi_1 + \phi_2)} \sin 2\theta_R \\
\langle \tilde{\chi}_{2R}^- | Z | \tilde{\chi}_{2R}^- \rangle &= -\frac{e}{s_W c_W} \left[s_W^2 - \frac{3}{4} + \frac{1}{4} \cos 2\theta_R \right]
\end{aligned} \tag{9}$$

where $s_W = \sin\theta_W$ is the weak angle. Note that every vertex here is an explicit function of φ_μ via the various mixing angles. However, the Z coupling to unlike charginos $\tilde{\chi}_i^+ \tilde{\chi}_j^-$ is manifestly complex, and its phase vanishes in the CP-conserving limit, $\varphi_\mu \rightarrow 0, \pi$.

Obviously, the photon vertex is independent of the SUSY phases

$$\langle \tilde{\chi}_{iL,R}^- | \gamma | \tilde{\chi}_{jL,R}^- \rangle = e\delta_{ij} \tag{10}$$

The process $q\bar{q} \rightarrow \tilde{\chi}_i^+ \tilde{\chi}_j^-$ is generated by the two mechanisms shown in Fig. 1. The s -channel γ and Z exchanges, and t -channel \tilde{q} exchange, where the latter is consistently neglected below. The transition amplitude can be parameterized as

$$T(q\bar{q} \rightarrow \tilde{\chi}_i^+ \tilde{\chi}_j^-) = \frac{e^2}{s} Q_{\alpha\beta} [\bar{v}(q) \gamma_\mu P_\alpha u(q)] [\bar{u}(\tilde{\chi}_i^-) \gamma^\mu P_\beta v(\tilde{\chi}_j^+)] \quad (11)$$

where the charges $Q_{\alpha\beta}$ are defined such that the first index corresponds to the chirality of the $\bar{q}q$ current and the second one to chargino current. For various final states, their expressions are given by

(i) $\underline{\tilde{\chi}_1^- \tilde{\chi}_1^+}$ for $\underline{q = u, c}$

$$\begin{aligned} Q_{LL} &= 1 + \frac{D_Z}{s_W^2 c_W^2} \left(\frac{1}{2} - \frac{2}{3} s_W^2 \right) \left(s_W^2 - \frac{3}{4} - \frac{1}{4} \cos 2\phi_L \right) \\ Q_{LR} &= 1 + \frac{D_Z}{s_W^2 c_W^2} \left(\frac{1}{2} - \frac{2}{3} s_W^2 \right) \left(s_W^2 - \frac{3}{4} - \frac{1}{4} \cos 2\phi_R \right) \\ Q_{RL} &= 1 + \frac{D_Z}{c_W^2} \left(-\frac{2}{3} \right) \left(s_W^2 - \frac{3}{4} - \frac{1}{4} \cos 2\phi_L \right) \\ Q_{RR} &= 1 + \frac{D_Z}{c_W^2} \left(-\frac{2}{3} \right) \left(s_W^2 - \frac{3}{4} - \frac{1}{4} \cos 2\phi_R \right) \end{aligned} \quad (12)$$

(ii) $\underline{\tilde{\chi}_1^- \tilde{\chi}_1^+}$ for $\underline{q = d, s}$

$$\begin{aligned} Q_{LL} &= 1 + \frac{D_Z}{s_W^2 c_W^2} \left(-\frac{1}{2} + \frac{1}{3} s_W^2 \right) \left(s_W^2 - \frac{3}{4} - \frac{1}{4} \cos 2\phi_L \right) \\ Q_{LR} &= 1 + \frac{D_Z}{s_W^2 c_W^2} \left(-\frac{1}{2} + \frac{1}{3} s_W^2 \right) \left(s_W^2 - \frac{3}{4} - \frac{1}{4} \cos 2\phi_R \right) \\ Q_{RL} &= 1 + \frac{D_Z}{c_W^2} \left(+\frac{1}{3} \right) \left(s_W^2 - \frac{3}{4} - \frac{1}{4} \cos 2\phi_L \right) \\ Q_{RR} &= 1 + \frac{D_Z}{c_W^2} \left(+\frac{1}{3} \right) \left(s_W^2 - \frac{3}{4} - \frac{1}{4} \cos 2\phi_R \right) \end{aligned} \quad (13)$$

(iii) $\underline{\tilde{\chi}_1^- \tilde{\chi}_2^+}$ for $\underline{q = u, c}$

$$Q_{LL} = \frac{D_Z}{4s_W^2 c_W^2} \left(\frac{1}{2} - \frac{2}{3} s_W^2 \right) e^{-i\phi_L} \sin 2\phi_L$$

$$\begin{aligned}
Q_{LR} &= \frac{D_Z}{4s_W^2 c_W^2} \left(\frac{1}{2} - \frac{2}{3} s_W^2 \right) e^{-i(\varphi_R - \phi_1 + \phi_2)} \sin 2\phi_R \\
Q_{RL} &= \frac{D_Z}{4c_W^2} \left(-\frac{2}{3} \right) e^{-i\varphi_L} \sin 2\phi_L \\
Q_{RR} &= \frac{D_Z}{4c_W^2} \left(-\frac{2}{3} \right) e^{-i(\varphi_R - \phi_1 + \phi_2)} \sin 2\phi_R
\end{aligned} \tag{14}$$

(iv) $\underline{\tilde{\chi}_1^- \tilde{\chi}_2^+}$ for $\underline{q = d, s}$

$$\begin{aligned}
Q_{LL} &= \frac{D_Z}{4s_W^2 c_W^2} \left(-\frac{1}{2} + \frac{1}{3} s_W^2 \right) e^{-i\varphi_L} \sin 2\phi_L \\
Q_{LR} &= \frac{D_Z}{4s_W^2 c_W^2} \left(-\frac{1}{2} + \frac{1}{3} s_W^2 \right) e^{-i(\varphi_R - \phi_1 + \phi_2)} \sin 2\phi_R \\
Q_{RL} &= \frac{D_Z}{4c_W^2} \left(+\frac{1}{3} \right) e^{-i\varphi_L} \sin 2\phi_L \\
Q_{RR} &= \frac{D_Z}{4c_W^2} \left(+\frac{1}{3} \right) e^{-i(\varphi_R - \phi_1 + \phi_2)} \sin 2\phi_R
\end{aligned} \tag{15}$$

(v) $\underline{\tilde{\chi}_2^- \tilde{\chi}_2^+}$ for $\underline{q = u, c}$

$$\begin{aligned}
Q_{LL} &= 1 + \frac{D_Z}{s_W^2 c_W^2} \left(\frac{1}{2} - \frac{2}{3} s_W^2 \right) \left(s_W^2 - \frac{3}{4} + \frac{1}{4} \cos 2\phi_L \right) \\
Q_{LR} &= 1 + \frac{D_Z}{s_W^2 c_W^2} \left(\frac{1}{2} - \frac{2}{3} s_W^2 \right) \left(s_W^2 - \frac{3}{4} + \frac{1}{4} \cos 2\phi_R \right) \\
Q_{RL} &= 1 + \frac{D_Z}{c_W^2} \left(-\frac{2}{3} \right) \left(s_W^2 - \frac{3}{4} + \frac{1}{4} \cos 2\phi_L \right) \\
Q_{RR} &= 1 + \frac{D_Z}{c_W^2} \left(-\frac{2}{3} \right) \left(s_W^2 - \frac{3}{4} + \frac{1}{4} \cos 2\phi_R \right)
\end{aligned} \tag{16}$$

(vi) $\underline{\tilde{\chi}_2^- \tilde{\chi}_2^+}$ for $\underline{q = d, s}$

$$\begin{aligned}
Q_{LL} &= 1 + \frac{D_Z}{s_W^2 c_W^2} \left(-\frac{1}{2} + \frac{1}{3} s_W^2\right) \left(s_W^2 - \frac{3}{4} + \frac{1}{4} \cos 2\phi_L\right) \\
Q_{LR} &= 1 + \frac{D_Z}{s_W^2 c_W^2} \left(-\frac{1}{2} + \frac{1}{3} s_W^2\right) \left(s_W^2 - \frac{3}{4} + \frac{1}{4} \cos 2\phi_R\right) \\
Q_{RL} &= 1 + \frac{D_Z}{c_W^2} \left(+\frac{1}{3}\right) \left(s_W^2 - \frac{3}{4} + \frac{1}{4} \cos 2\phi_L\right) \\
Q_{RR} &= 1 + \frac{D_Z}{c_W^2} \left(+\frac{1}{3}\right) \left(s_W^2 - \frac{3}{4} + \frac{1}{4} \cos 2\phi_R\right)
\end{aligned} \tag{17}$$

Here all the amplitudes are built up by the γ and Z exchanges, and $D(Z)$ stands for the Z propagator: $D_Z = \hat{s}/(\hat{s} - m_Z^2 + im_Z \Gamma_Z)$.

In what follows, for convenience we will introduce four combinations of the charges

$$\begin{aligned}
Q_1 &= \frac{1}{4} [|Q_{RR}|^2 + |Q_{LL}|^2 + |Q_{RL}|^2 + |Q_{LR}|^2] \\
Q_2 &= \frac{1}{2} \text{Re} [Q_{RR} Q_{RL}^* + Q_{LL} Q_{LR}^*] \\
Q_3 &= \frac{1}{4} [|Q_{RR}|^2 + |Q_{LL}|^2 - |Q_{RL}|^2 - |Q_{LR}|^2] \\
Q_4 &= \frac{1}{2} \text{Im} [Q_{RR} Q_{RL}^* + Q_{LL} Q_{LR}^*]
\end{aligned} \tag{18}$$

so that the differential cross section can be expressed simply as

$$\frac{d\hat{\sigma}}{d \cos \Theta} (q\bar{q} \rightarrow \tilde{\chi}_i^+ \tilde{\chi}_j^-) = \frac{\pi \alpha^2}{2\hat{s}} \lambda^{1/2} \{ [1 - (\mu_i^2 - \mu_j^2)^2 + \lambda \cos^2 \Theta] Q_1 + 4\mu_i \mu_j Q_2 + 2\lambda^{1/2} Q_3 \cos \Theta \} \tag{19}$$

with the usual two body phase space factor

$$\lambda(1, \mu_i^2, \mu_j^2) = [1 - (\mu_i + \mu_j)^2][1 - (\mu_i - \mu_j)^2] \tag{20}$$

defined via the reduced mass $\mu_i^2 = \frac{m_{\tilde{\chi}_i^\pm}^2}{\hat{s}}$.

Integrating the differential cross section over the center-of-mass scattering angle Θ one can obtain the total partonic cross section

$$\hat{\sigma} = \hat{\sigma}(\varphi_\mu, \mu, M_2, \hat{s}, \tan \beta) \quad (21)$$

whose dependence on φ_μ , M_2 and $|\mu|$ will be analyzed numerically.

The total cross section for the chargino-pair production through $q\bar{q}$ fusion at the LHC center of mass energy $\sqrt{s} = 14$ TeV, can be obtained by integrating partonic cross section $\hat{\sigma}$, over the quark-antiquark luminosities in the distribution function of proton, which is given in parton model by the formula [10]

$$\sigma(pp \rightarrow q\bar{q} \rightarrow \tilde{\chi}_i^+ \tilde{\chi}_j^- + X) = \int_{\frac{Q^2}{s}}^1 d\tau \frac{d\mathcal{L}_{q\bar{q}}}{d\tau} \hat{\sigma}_{q\bar{q}}(q\bar{q} \rightarrow \tilde{\chi}_i^+ \tilde{\chi}_j^-, \text{ at } \hat{s} = \tau s) \quad (22)$$

with a quark luminosity in proton which is defined as

$$\frac{d\mathcal{L}_{q\bar{q}}}{d\tau} = \int_{\tau}^1 \frac{dx_A}{x_A} \sum_{ij=q,\bar{q}} f_{i/A}(x_A, Q^2) f_{j/B}(x_B, Q^2) \quad (23)$$

where $f_{i/A}(x_A, Q^2)$ are the parton distribution functions for parton i in hadron A with momentum fraction x_A evaluated at the factorization scale $Q^2 = (m_{\tilde{\chi}_i^+} + m_{\tilde{\chi}_j^+})^2$, and $\tau = x_A x_B$. Here, s is the hadron-hadron center of mass energy squared which is related to \hat{s} , the parton-parton center of mass energy squared, via $\hat{s} = x_A x_B s$.

To calculate the total cross sections for LHC, one has to know parton distributions as functions of the scaling variables $x_{A,B}$ and Q^2 . Although the distributions have not been measured at such values of Q^2 , one can obtain them using Altarelli-Parisi equation [9] and the parton distributions at some scale Q_0^2 . For this purpose, we used CTEQ4M parton densities, without any QCD corrections for simplicity in our analysis [11].

These results are illustrated in Figs. 2-4, where the production cross-section is plotted against the phase angle at the LHC with $\sqrt{s} = 14$ TeV.

Besides these, it is necessary to analyze the rate asymmetries for having a better information about φ_μ .

Analyzing the effects due to normal polarization of the charginos, the CP-violating phase φ_μ can be determined. Concerning this point, we investigate the normal polarization vector

of the charginos which are inherently CP-odd and therefore exist if CP is broken in the fundamental theory. The normal polarization vector is defined as

$$P_N = 8\lambda^{1/2}\mu_j \sin \Theta \frac{Q_4}{N} \quad (24)$$

for $\tilde{\chi}_j^+ \tilde{\chi}_j^-$, the j -th chargino, and it is defined as

$$P_N[\tilde{\chi}_{i,j}^\pm] = \pm 4\lambda^{1/2}\mu_{j,i}(F_R^2 - F_L^2) \sin \Theta \sin 2\phi_L \\ \times \sin 2\phi_R \sin(\beta_L - \beta_R + \gamma_1 - \gamma_2)/N \quad (25)$$

for non-diagonal pairs $\tilde{\chi}_i^+ \tilde{\chi}_j^-$ where $i \neq j$. Here

$$N = 4[(1 - (\mu_i^2 - \mu_j^2)^2 + \lambda \cos^2 \Theta)Q_1 + 4\mu_i\mu_j Q_2 + 2\lambda^{1/2}Q_3 \cos \Theta] \quad (26)$$

and

$$F_R = \frac{D_Z}{4c_W^2}, \quad F_L = \frac{D_Z}{4s_W^2 c_W^2} (s_W^2 - \frac{1}{2}). \quad (27)$$

A non-vanishing P_N will be sufficient to establish non-vanishing CP violation in the system. Therefore, the value of non-vanishing P_N implies the strength of the CP invariance breaking in SUSY.

III. NUMERICAL ESTIMATES

In this section we will discuss the dependence of the chargino production cross section on φ_μ , M_2 and $|\mu|$ at $\sqrt{s} = 14$ TeV. We apply everywhere the existing collider constraint that $m_{\chi_2} > 104$ GeV.

In Table 1, we give the cross section values for $pp \rightarrow \tilde{\chi}_1^+ \tilde{\chi}_1^- + X$ and $pp \rightarrow \tilde{\chi}_1^+ \tilde{\chi}_2^- + X$ taking $M_2 = 150, 300$ GeV, $\mu = 150, 300$ GeV, $\tan \beta = 4, 10, 30, 50$, and $\varphi_\mu = \pi/3$ in the calculations.

In Figs. 2 and 3 we show the dependence of the cross sections $pp \rightarrow \tilde{\chi}_1^+ \tilde{\chi}_1^- + X$ and $pp \rightarrow \tilde{\chi}_1^+ \tilde{\chi}_2^- + X$ on φ_μ , for $M_2 = 150, 300$ GeV, $\mu = 150, 300$ GeV, and $\tan\beta = 10$.

The variation of the cross section makes it clear that, as φ_μ varies from 0 to π the cross section decreases gradually. The more spectacular enhancement implies the lighter chargino mass.

The decrease of the cross section is tied up to the variation of the chargino masses with the phases. It is clear that as $\varphi_\mu : 0 \rightarrow \pi$ the mass splitting of the charginos decrease. This is an important effect which implies that the cross section is larger than what one would expect from the CP-conserving theory [7].

Apart from the cross section itself, one can analyze various spin and charge asymmetries which are expected to have an enhanced dependence on φ_μ . The normal polarization in $q\bar{q} \rightarrow \tilde{\chi}_1^+ \tilde{\chi}_1^-$ is zero since the $\tilde{\chi}_1^+ \tilde{\chi}_1^- \gamma$ and $\tilde{\chi}_1^+ \tilde{\chi}_1^- Z$ vertices are real even for non-zero phases in the chargino mass matrix.

In Fig. 6 we show the normal polarization P_N of unlike charginos in $q\bar{q} \rightarrow \tilde{\chi}_1^+ \tilde{\chi}_2^-$ which has a different dependence on the phases. Here again $M_2 = 150, 300$ GeV, $\mu = 150, 300$ GeV, $\tan\beta = 10$, and $\varphi_\mu = \pi/2$. The value of φ_μ is chosen since the normal polarization is maximum at $\varphi_\mu = \pi/2$. This result will be discussed in the next section.

The dependence of the normal polarization on the value of Θ and φ_μ is shown in Fig. 7, where the normal polarization has its maximum at $\Theta = \pi/2$ as expected from the Equation 24, and at $\varphi_\mu = \pi/2$ as stated above.

We believe that for clarifying the essence of measuring φ_μ the first quantity to be tested is the cross section itself.

IV. DISCUSSION AND CONCLUSION

We have analyzed the production of chargino pairs at LHC energies at the aim of isolating the phase of the μ parameter. Our results (Figs. 2-3) suggest that, there is a strong dependence on the phase of the μ parameter. The cross section is minimum for the value of the phase $\varphi_\mu = \pi$. This result is understandable since the mass of the lightest (heaviest) chargino makes a maximum (minimum) at this point. It is particularly clear that $\chi_1^+ \chi_1^-$ production rate is depleted in this region. The size and dependence on φ_μ of the cross section both get enhanced for small enough soft masses, *i.e.* $M_2=150$ GeV and $\mu=150$ GeV. As an example, this is seen for the value of $\varphi_\mu = \pi$, $m_{\chi_1} = 111$ GeV when $M_2=150$ GeV and $\mu=150$ GeV and for the same value of φ_μ , $m_{\chi_1} = 142$ GeV when $M_2=150$ GeV and $\mu=300$ GeV. The physical chargino mass increases as the values of M_2 and μ increase.

The cross section values that we have obtained for $pp \rightarrow \tilde{\chi}_1^+ \tilde{\chi}_1^- + X$ process at the LHC can reach a few 10 fb, whereas for the $\tilde{\chi}_1^+ \tilde{\chi}_2^-$ pair productions, the cross sections are in the range of a few fb. Having an annual luminosity of 100 fb⁻¹, one may accumulate 10³ and 100 events per year for $\tilde{\chi}_1^+ \tilde{\chi}_1^-$ and $\tilde{\chi}_1^+ \tilde{\chi}_2^-$ pair productions respectively. This is a hard task to obtain a clean signature, but the measurement of these processes will be an important step for determining the CP violation sources of low-energy supersymmetry.

The cross sections of the subprocess $q\bar{q} \rightarrow \tilde{\chi}_1^+ \tilde{\chi}_1^-$ and $q\bar{q} \rightarrow \tilde{\chi}_1^+ \tilde{\chi}_2^-$ as a function of $q\bar{q}$ c.m.s. energy $\sqrt{\hat{s}}$ are depicted in Figs. 4 and 5. There are sharp rising peaks around $\sqrt{\hat{s}} \sim 300$ GeV and $\sqrt{\hat{s}} \sim 500$ GeV for $\tilde{\chi}_1^+ \tilde{\chi}_1^-$ and $\tilde{\chi}_1^+ \tilde{\chi}_2^-$ respectively, due to the threshold conditions $\sqrt{\hat{s}} \sim m_{\tilde{\chi}_i^\pm} + m_{\tilde{\chi}_j^\pm}$ (i,j=1,2).

Since the cross sections for $q\bar{q} \rightarrow \tilde{\chi}_i^+ \tilde{\chi}_j^-$ have their peaks at the energies less than 1 TeV, the upgraded Tevatron as well, with a c.m.s energy of 1.8 TeV and 30 fb⁻¹ integrated luminosity, is a useful machine to detect CP violation of SUSY particles. In fact, it is more likely to see chargino pairs at such $p\bar{p}$ colliders than at the LHC. This follows from the fact that the anti-quarks needed for chargino pair production are always drained from the sea

for pp colliders. In this sense our analysis puts a lower bound on the likelihood of observing chargino pairs at hadron colliders. In this respect, the proton-antiproton collider Tevatron and, to a greater extent, the proton-proton collider LHC, are the almost ideal places of probing such a minimal SUSY scenario of explicit CP violation.

In Fig. 6, we show the dependence of the normal polarization of $q\bar{q} \rightarrow \tilde{\chi}_1^+ \tilde{\chi}_2^-$ on Θ , for $M_2 = 150, 300$ GeV, $\mu = 150, 300$ GeV, and $\tan\beta = 10$. As seen from the figure, P_N is not vanishing for masses of lighter charginos, and this is an indication of the CP invariance breaking in SUSY. For the higher values of M_2 and μ , P_N is practically vanishing as the mass of charginos increases.

In true experimental environment, the cross sections we have studied are for subprocess obtained by integration over appropriate structure functions. However, given the energy span of LHC that it will be possible to probe sparticles up to 2 TeV, it is clear that the center-of-mass energies we discuss are always within the experimental reach. If the experiment concludes $\varphi_\mu \sim \mathcal{O}(1)$ then, given strong bounds from the absence of permanent EDMs for electron, neutron, atoms and molecules, one would conclude that the first two generations of sfermions will be hierarchically split from the ones in the third generation. In case the experiment reports a small φ_μ then presumably all sfermion generations can lie right at the weak scale in agreement with the EDM bounds. In this case, where φ_μ is a small fraction of π , one might expect that the minimal model is UV-completed above the TeV scale such that the μ parameter is promoted to a dynamical SM-singlet field (*e.g.* the Z' models).

FIGURE CAPTIONS

FIGURE 1. The lowest order Feynman diagrams for $q\bar{q} \rightarrow \tilde{\chi}_i^+ \tilde{\chi}_j^-$ processes.

FIGURE 2. The plot of cross section for $pp \rightarrow \tilde{\chi}_1^+ \tilde{\chi}_1^- + X$ as a function of φ_μ for the values of $\mu = 150, 300$ GeV, $M_2 = 150, 300$ GeV and $\tan \beta = 10$.

FIGURE 3. The plot of cross section for $pp \rightarrow \tilde{\chi}_1^+ \tilde{\chi}_2^- + X$ as a function of φ_μ for the values of $\mu = 150, 300$ GeV, $M_2 = 150, 300$ GeV, and $\tan \beta = 10$.

FIGURE 4. The plot of cross section for $q\bar{q} \rightarrow \tilde{\chi}_1^+ \tilde{\chi}_1^-$ versus the c.m.s. energy of incoming quarks $\sqrt{\hat{s}}$ for the values of $\varphi_\mu = 0$, $\mu = 150, 300$ GeV, $M_2 = 150, 300$ GeV and $\tan \beta = 10$.

FIGURE 5. The plot of cross section for $q\bar{q} \rightarrow \tilde{\chi}_1^+ \tilde{\chi}_2^-$ versus the c.m.s. energy of incoming quarks $\sqrt{\hat{s}}$ for the values of $\varphi_\mu = 0$, $\mu = 150, 300$ GeV, $M_2 = 150, 300$ GeV and $\tan \beta = 10$.

FIGURES 6. The plot of normal polarization for $q\bar{q} \rightarrow \tilde{\chi}_1^+ \tilde{\chi}_2^-$ as a function of Θ for the values of $\mu = 150, 300$ GeV, $M_2 = 150, 300$ GeV and $\tan \beta = 10$, when $\varphi_\mu = \pi/2$.

FIGURES 7. 3-dimensional plot of normal polarization for $q\bar{q} \rightarrow \tilde{\chi}_1^+ \tilde{\chi}_2^-$ as a function of Θ and φ_μ for the values of $\mu = 150$ GeV, $M_2 = 150$ GeV and $\tan \beta = 10$.

REFERENCES

- [1] F. Gabbiani, E. Gabrielli, A. Masiero and L. Silvestrini, Nucl. Phys. B **477**, 321 (1996) [arXiv:hep-ph/9604387].
- [2] V. D. Barger, T. Falk, T. Han, J. Jiang, T. Li and T. Plehn, Phys. Rev. D **64**, 056007 (2001) [arXiv:hep-ph/0101106].
- [3] D. A. Demir and M. B. Voloshin, Phys. Rev. D **63**, 115011 (2001) [arXiv:hep-ph/0012123].
- [4] D. A. Demir, A. Masiero and O. Vives, Phys. Rev. D **61**, 075009 (2000) [arXiv:hep-ph/9909325]; Phys. Rev. Lett. **82**, 2447 (1999) [arXiv:hep-ph/9812337]; S. w. Baek, J. H. Jang, P. Ko and J. H. Park, Phys. Rev. D **62**, 117701 (2000) [arXiv:hep-ph/9907572]; S. w. Baek and P. Ko, Phys. Rev. Lett. **83**, 488 (1999) [arXiv:hep-ph/9812229]; D. A. Demir and K. A. Olive, Phys. Rev. D **65**, 034007 (2002) [arXiv:hep-ph/0107329]; M. Boz and N. K. Pak, Phys. Lett. B **531**, 119 (2002) [arXiv:hep-ph/0201199].
- [5] D. A. Demir, Phys. Rev. D **60**, 055006 (1999) [arXiv:hep-ph/9901389]; A. Pilaftsis and C. E. Wagner, Nucl. Phys. B **553**, 3 (1999) [arXiv:hep-ph/9902371]; T. Ibrahim and P. Nath, Phys. Rev. D **63**, 035009 (2001) [arXiv:hep-ph/0008237].
- [6] D. A. Demir, Phys. Lett. B **465**, 177 (1999) [arXiv:hep-ph/9809360]; G. L. Kane and L. T. Wang, Phys. Lett. B **488**, 383 (2000) [arXiv:hep-ph/0003198].
- [7] V. D. Barger, T. Han, T. J. Li and T. Plehn, Phys. Lett. B **475**, 342 (2000) [arXiv:hep-ph/9907425]; S. Y. Choi, J. Kalinowski, G. Moortgat-Pick and P. M. Zerwas, Eur. Phys. J. C **22**, 563 (2001) [Addendum-ibid. C **23**, 769 (2002)] [arXiv:hep-ph/0108117]; S. Y. Choi, A. Djouadi, M. Guchait, J. Kalinowski, H. S. Song and P. M. Zerwas, Eur. Phys. J. C **14**, 535 (2000) [arXiv:hep-ph/0002033]; Phys. Lett. B **479**, 235 (2000) [arXiv:hep-ph/0001175]; S. Y. Choi, A. Djouadi, H. S. Song and P. M. Zerwas, Eur.

- Phys. J. C **8**, 669 (1999) [arXiv:hep-ph/9812236]; S. Y. Choi, A. Djouadi, H. K. Dreiner, J. Kalinowski and P. M. Zerwas, Eur. Phys. J. C **7**, 123 (1999) [arXiv:hep-ph/9806279].
- [8] L. Kneur and G. Moultaka,
Phys. Rev. D **61**, 095003 (2000) [arXiv:hep-ph/9907360]; D. A. Demir, Phys. Rev. D **60**, 095007 (1999) [arXiv:hep-ph/9905571]; P. Nath, Phys. Rev. Lett. **66**, 2565 (1991).
- [9] Altarelli, G., and G. Parisi, 1977, Nucl. Phys. B126, 29.
- [10] S.M.Berman, J.D.Bjorken and J.B.Kogut, Phys.Rev.D4(1971)3388; E.Eichten, I.Hinchliffe, K.Lane and C.Quigg, Rev.Mod.Phys.56(1984)579; E58,1065(1986)
- [11] H. L. Lai et al. (CTEQ Collaboration), Phys. Rev. D 55, 1280 (1997).

TABLES

TABLE I. The cross section values for $pp \rightarrow \tilde{\chi}_1^+ \tilde{\chi}_1^- + X$ and $pp \rightarrow \tilde{\chi}_1^+ \tilde{\chi}_2^- + X$ processes for $\varphi_\mu = \pi/3$, $\mu = 150, 300$ GeV, $M_2 = 150, 300$ GeV, and $\tan\beta = 4, 10, 30, 50$.

$\tan\beta$	$M_2(\text{GeV})$	$\mu(\text{GeV})$	$\sigma(pp \rightarrow \tilde{\chi}_1^+ \tilde{\chi}_1^- + X)(\text{pb})$	$\sigma(pp \rightarrow \tilde{\chi}_1^+ \tilde{\chi}_2^- + X)(\text{fb})$
4	150	150	0.071	2.17
4	150	300	0.056	0.50
4	300	150	0.032	0.50
4	300	300	0.015	0.67
10	150	150	0.067	2.09
10	150	300	0.054	0.46
10	300	150	0.031	0.46
10	300	300	0.014	0.66
30	150	150	0.065	2.06
30	150	300	0.053	0.45
30	300	150	0.03	0.45
30	300	300	0.014	0.66
50	150	150	0.064	2.05
50	150	300	0.052	0.45
50	300	150	0.030	0.45
50	300	300	0.013	0.66

FIGURES

FIG. 1. The lowest order Feynman diagrams for $q\bar{q} \rightarrow \tilde{\chi}_i^+ \tilde{\chi}_j^-$ processes.

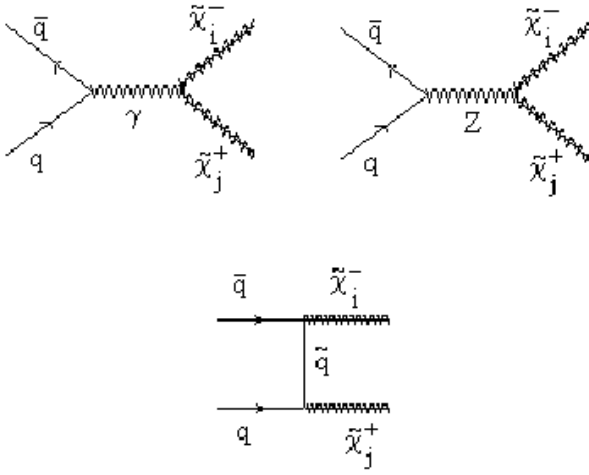


FIG. 2. The plot of cross section for $pp \rightarrow \tilde{\chi}_1^+ \tilde{\chi}_1^- + X$ as a function of φ_μ for the values of $\mu = 150, 300$ GeV, $M_2 = 150, 300$ GeV and $\tan\beta = 10$.

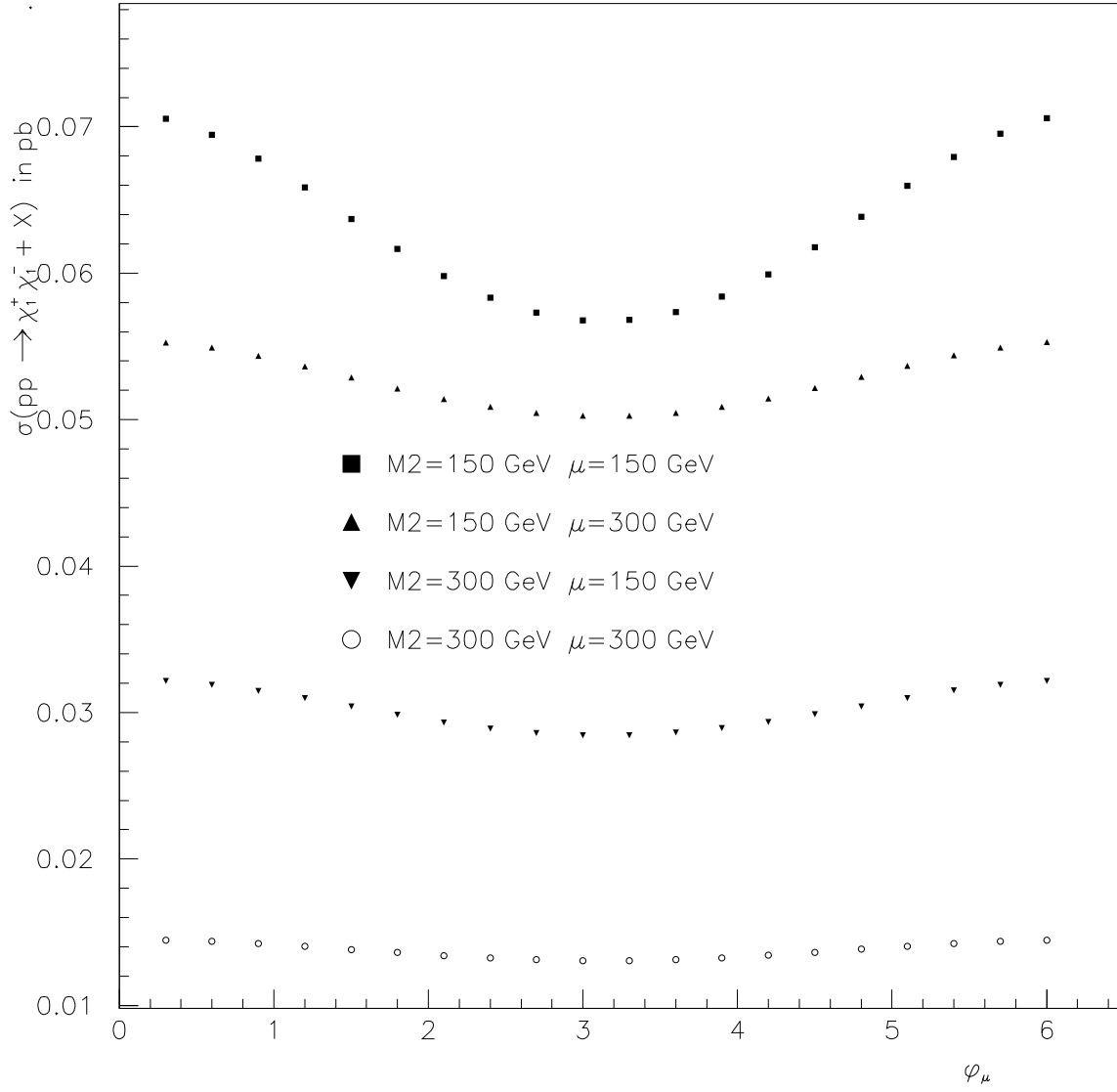


FIG. 3. The plot of cross section for $pp \rightarrow \tilde{\chi}_1^+ \tilde{\chi}_2^- + X$ as a function of φ_μ for the values of $\mu = 150, 300$ GeV, $M_2 = 150, 300$ GeV and $\tan\beta = 10$.

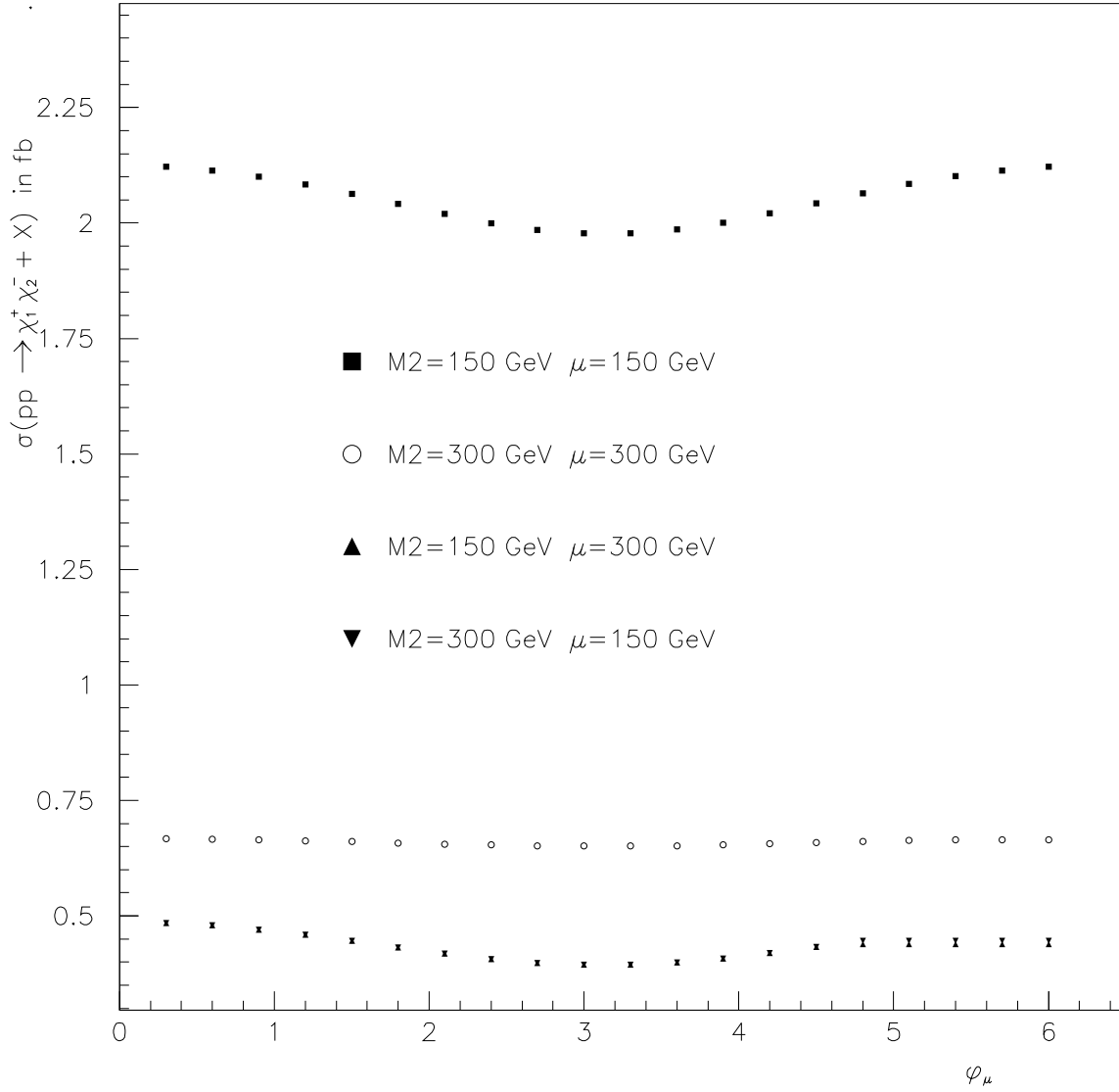


FIG. 4. The cross sections of the subprocess $q\bar{q} \rightarrow \tilde{\chi}_1^+ \tilde{\chi}_1^-$ versus the c.m.s. energy of incoming quarks $\sqrt{\hat{s}}$ for the values of $\varphi_\mu = 0$, $\mu = 150, 300$ GeV, $M_2 = 150, 300$ GeV and $\tan\beta = 10$.

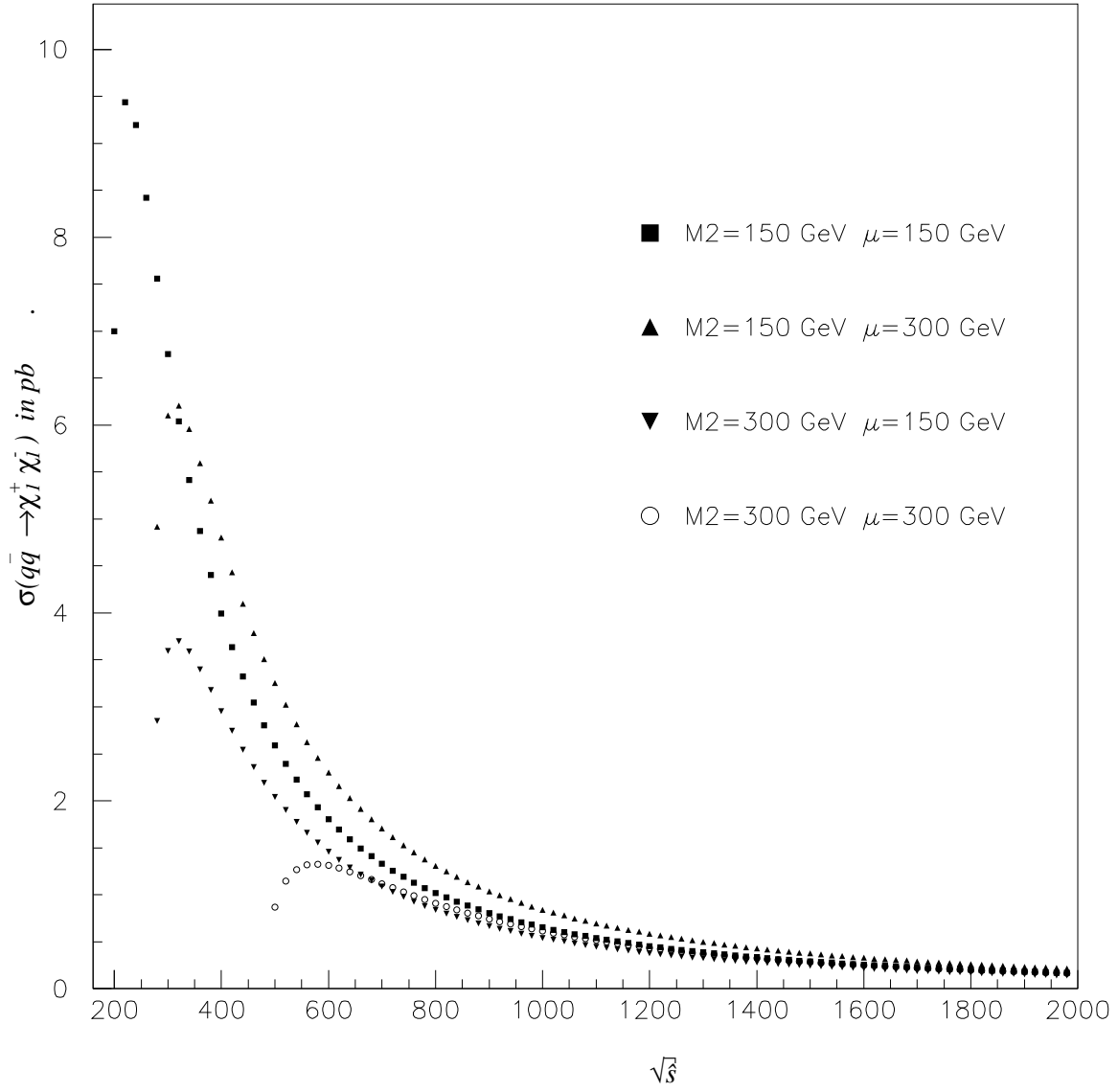


FIG. 5. The cross sections of the subprocess $q\bar{q} \rightarrow \tilde{\chi}_1^+ \tilde{\chi}_2^-$ versus the c.m.s. energy of incoming quarks $\sqrt{\hat{s}}$ for the values of $\varphi_\mu = 0, \mu = 150, 300$ GeV, $M_2 = 150, 300$ GeV and $\tan \beta = 10$.

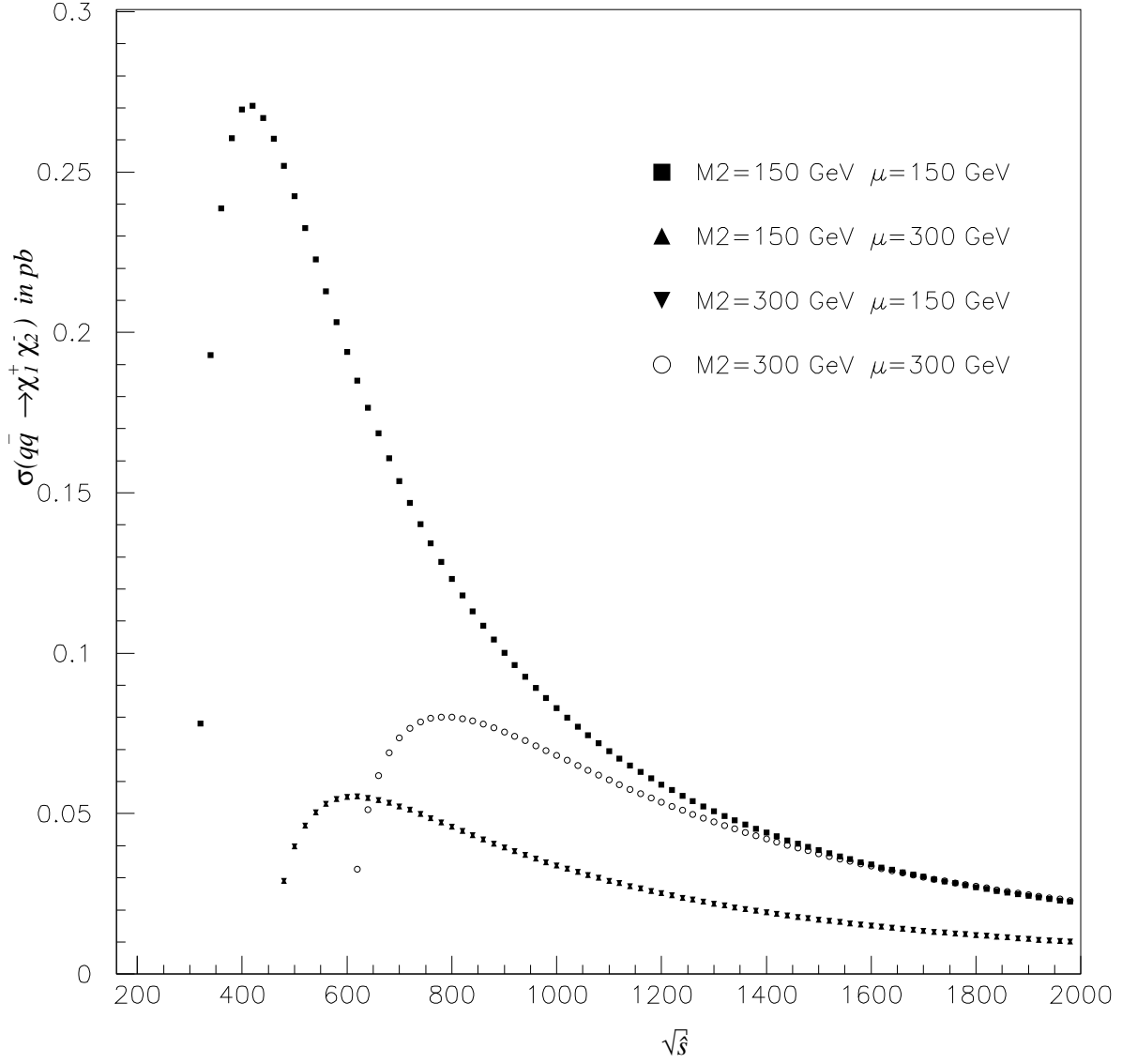


FIG. 6. The plot of normal polarization for $q\bar{q} \rightarrow \tilde{\chi}_1^+ \tilde{\chi}_2^-$ as a function of Θ for the values of $\mu = 150, 300$ GeV, $M_2 = 150, 300$ GeV, $\tan\beta = 10$ and $\varphi_\mu = \pi/2$.

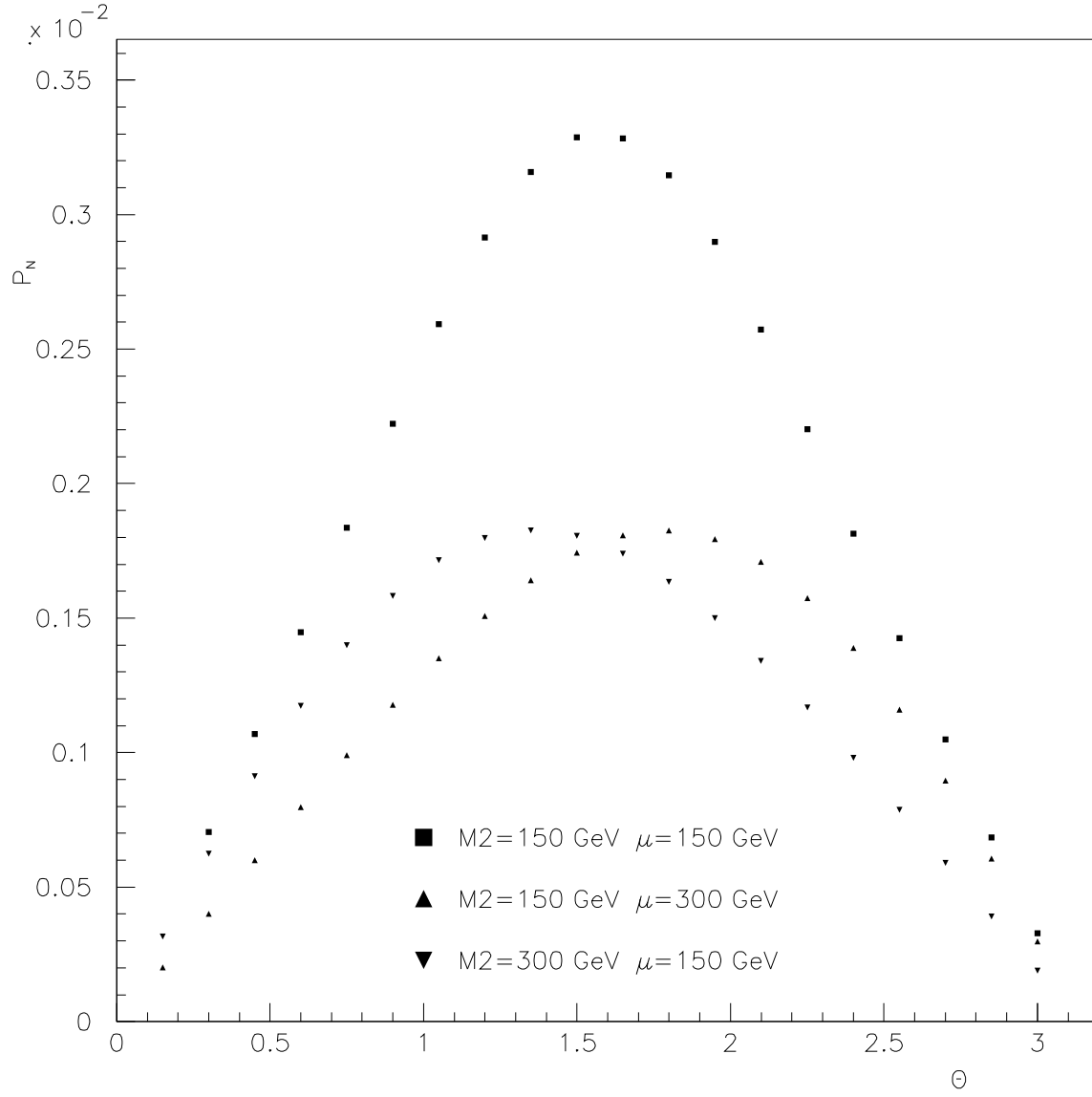


FIG. 7. The plot of normal polarization for $q\bar{q} \rightarrow \tilde{\chi}_1^+ \tilde{\chi}_2^-$ as a function of Θ and φ_μ for the values of $\mu = 150$ GeV, $M_2 = 150$ GeV and $\tan\beta = 10$.

